OPTIMAL RASTERING ORIENTATION IN FREEFORM EXTRUSION FABRICATION PROCESSES

Amir Ghazanfari, Wenbin Li, Ming C. Leu, and Robert G. Landers

Mechanical and Aerospace Engineering Department
Missouri University of Science and Technology, Rolla, MO, USA

REVIEWED

Abstract

Many researchers have tried to optimize the build direction of additively manufactured parts to minimize the vertical staircase effect. However, the horizontal staircase effect should also be considered when fully dense parts are to be fabricated. In this paper, part inaccuracy due to the horizontal staircase effect is considered in order to determine the optimal rastering orientation in building the part. An algorithm is developed to estimate this inaccuracy and a technique is proposed to minimize it. The effect of rastering orientation on staircase errors is examined, and the particle swarm optimization method is used to determine the optimum rastering angle that leads to minimum errors for each layer. Several case studies are considered where the staircase errors are calculated with and without optimizing the rastering orientation. The results show that the errors can be reduced considerably when using the optimal rastering orientation. To verify the analytical results, parts are fabricated using a freeform extrusion fabrication process at various angles and the errors are compared.

Introduction

Dimensional accuracy has always been an important challenge in all additive manufacturing technologies [1]. The inaccuracy is a result of employing lines of deposited material to approximate the complex shape of a part. This phenomenon is frequently called the staircase effect. When this effect occurs between adjacent layers, it is referred to as “vertical staircase effect” and if it is between contiguous lines in a layer, the term “horizontal staircase effect” is used. One way to reduce this effect is decreasing the size of the line which will patently protract the fabrication process as well. An efficacious scheme used to reduce the “vertical” staircase effect is optimizing the deposition orientation. Many researchers have employed different optimization methods to achieve this aim considering various objective functions and constraints.

Cheng et al. [2] considered accuracy as the primary objective and productivity as the secondary objective in stereolithography and proposed a method to determine an optimum deposition orientation. Productivity was increased by reducing the number of layers. First, orientations resulting in low error values were chosen and among them, the one leading to the shortest fabrication time was selected. Alexander et al. [3] optimized part accuracy and cost in stereolithography and fused deposition modeling by determining the deposition orientation. They selected average weighted cusp height as a measure of accuracy and proposed models to predict cost as a function of orientation for the two processes. Thrimurthulu et al. [4] obtained an optimum deposition orientation for the fused deposition modeling process, which enhanced part surface finish and reduced build time. Models for evaluation of average part surface roughness and build time were developed and a real-coded genetic algorithm was used to obtain the optimum solution.

Canellidis et al. [5] proposed a framework that constitutes two independent modules. The first module evaluates how “good” a randomly selected orientation is by assessing the fabrication time, defined as build time plus post-processing time, as the main cost/time criterion and the part’s average surface roughness as the overall quality criterion. The combined effect of the two criteria was evaluated through a weighted multi-criteria objective function. Phatak and Pande [6] sliced a CAD model of the part and hollowed it with the desired shell thickness. A genetic algorithm based strategy was then used to obtain the optimum part orientation. The objective of optimization was a weighted average of performance measures such as build time, part quality, and the material used in the hollowed model.

Paul and Anand [7] examined the relationship between cylindricity form error and build orientation using three methods: a simple analytical model, the CAD model of the part, and the STL file of the part. The results were then used to obtain the critical orientation zones that minimize the cylindricity error for a part. The method was demonstrated by determining the optimal orientation zones of a test part with multiple cylindrical features. In another paper [8], they also analyzed the effect of part orientation on cylindricity and flatness form errors. An algorithm to calculate the optimal orientation for minimizing flatness and cylindricity errors was developed and tested. They noticed that an optimal orientation for minimum form errors may result in a greater utilization of support structures. Thus, they tried to minimize the volume of support structures while minimizing the cylindricity and flatness errors.

The most common practical approach to reduce the horizontal errors is surrounding the inner rasters by outer contours. However, although this approach improves the surface finish, it introduces gaps between the outer contours and inner rasters. These gaps affect the mechanical properties of the part, especially if the part is to be made of ceramic materials which are very sensitive to imperfections. In this paper, the horizontal staircase effect is minimized by optimizing the rastering orientation for each individual layer. An algorithm is developed to estimate the error and the Particle Swarm Optimization (PSO) method is used to find the rastering orientation which results in minimum error. One of the designed parts is fabricated via a freeform extrusion fabrication process to verify the analytical results.

Error estimation algorithm

As shown in Figure 1, each layer is composed of parallel lines with a constant width and a constant thickness. Since in the fabrication process the material is extruded through a circular nozzle, the lines are assumed to have a circular end shape. Their length is limited between the part's stl file boundary such that the midline intersects with the stl boundary at both ends (shown by the blue points in Figure 1).

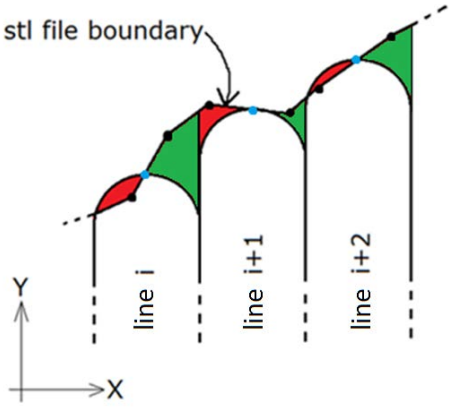

Figure 1. Stl file boundary and parallel lines forming a layer. Areas between lines and the stl file boundary filled with red and green colors are a measure of staircase error.

To estimate the staircase error for each line, the areas between the stl file boundary and line boundary are calculated and assumed to be a measure of error. There are four error values for each line (two at one end as shown in red and green colors in Figure 1, and two at the other end not shown in the figure) and the maximum of the four values is considered to be the error for that line. To calculate the four areas for each line, a numerical integration technique (trapezoidal rule) is employed. Each area can be obtained using

$$A_{ij} = \int_{x_0}^{x_0+w} |f(x) - g(x)|dx = \frac{w}{4N}\sum_{k=1}^{N}|f(x_{k+1}) - g(x_{k+1})| + |f(x_k) - g(x_k)| \quad (1)$$

where A_{ij} is the j^{th} (j = 1,2,3,4) area corresponding to the i^{th} line, x_0 corresponds to the left edge of the line, w is the line width, f represents the stl file boundary, g is the line boundary, and N is the number of equally spaced integration panels. The lines could be along any direction, but the same procedure is used to calculate the areas by rotating the coordinate system so that the Y direction is along the line's direction.

Since each layer is composed of a finite number of lines, an error diagram for each layer could be plotted by calculating the error for each line. A program is written in MATLAB which reads the geometry of the part from a CAD file in stl format, finds the intersections of the representative surfaces of the part with horizontal planes and forms the boundary for each layer. After the layer boundary is obtained from the stl file, rastering will be performed to fill in the desired area with lines for the layer. Figure 2 shows the rastering and error diagrams for a layer of an arbitrary object rastered with lines of 0.9 mm width. Each error value corresponds to one line and each line is represented by a straight line passing through its center.

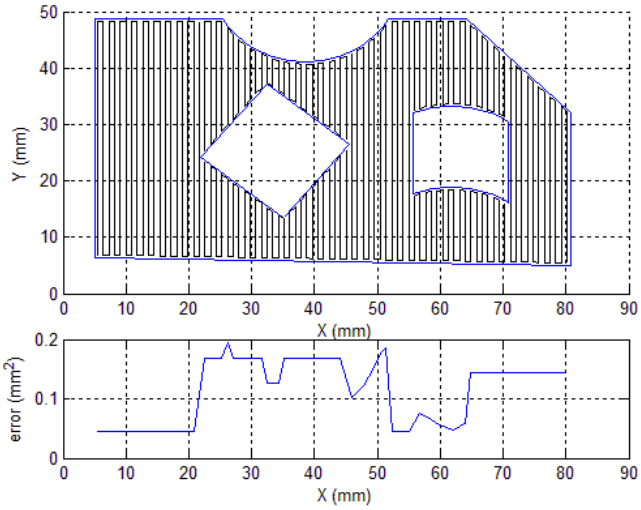

Figure 2. Rastering and error diagram for a layer of an arbitrary object rastered with 0.9 mm wide lines.

By changing the rastering orientation of the layer, the errors change significantly as shown in Figure 3, where an arbitrary shape rastered with lines of 0.9 mm width is rotated 45° CCW. The rotation results in a 33.7% reduction in maximum error while the fabrication time remains constant. Thus, developing an optimization algorithm to find the optimum rastering orientation could result in a considerable improvement in part accuracy without sacrificing productivity.

Particle Swarm Optimization

Kennedy and Eberhart [9] introduced the Particle Swarm Optimization (PSO) method, which is an evolutionary computational technique based on swarm intelligence. In this method, each candidate solution to the optimization problem is considered as the trajectory of a particle and is adjusted in the search space based on the experience of its own as well as other particles in the swarm. It is assumed that there are N particles in the swarm and the particles can move in a D-dimensional search space. The set of parameters in the i^{th} iteration are represented by the position vector of the j^{th} particle, $\boldsymbol{X}_j^i = (x_{j1}^i, x_{j2}^i, \dots, x_{jD}^i)$, and changes in the parameters are represented by velocity of the particle, $\boldsymbol{V}_j^i = (v_{j1}^i, v_{j2}^i, \dots, v_{jD}^i)$. Initially, the N particles are randomly distributed in the space and finally all of them will reach the optimal point.

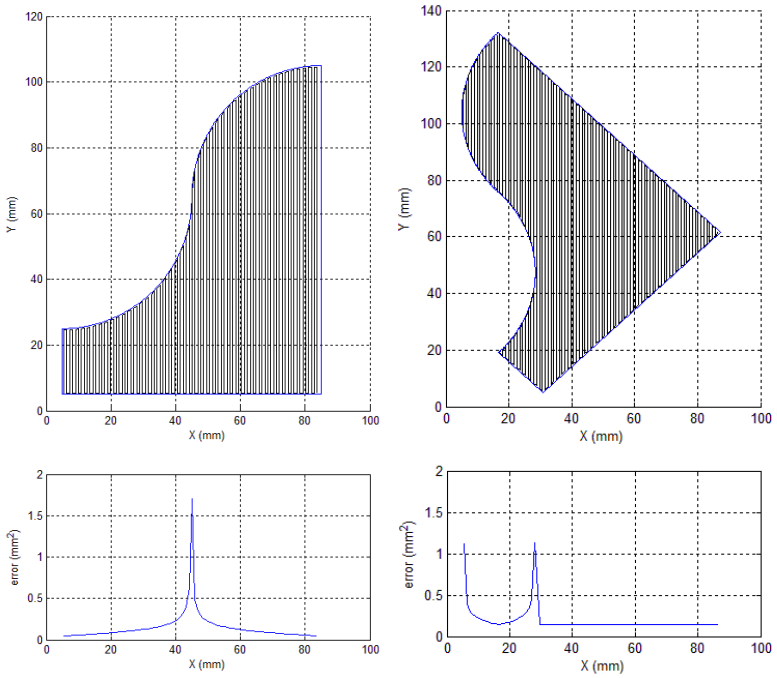

Figure 3. An arbitrary shape rastered at two different orientations along with the error daigram for each orientation.

The key step in PSO is calculating the velocity of each particle at each iteration. This velocity depends on the previous velocity of the particle, the historical best value for the particle, and the historical best value of all particles as follows:

$$\boldsymbol{V}_j^i = \theta \boldsymbol{V}_j^{i-1} + c_1 r_1 [\boldsymbol{P}_{best,j} - \boldsymbol{X}_j^{i-1}] + c_2 r_2 [\boldsymbol{G}_{best} - \boldsymbol{X}_j^{i-1}] \tag{2}$$

where $\boldsymbol{P}_{best,j}$ is the position of j^{th} particle corresponding to the best value of the objective function encountered by this particle in all the previous iterations; $\boldsymbol{G}_{best}$ is the position of the particle experiencing the best value of the objective function encountered in the previous iterations by any of the N particles; c_1 and c_2 are the cognitive (individual) and social (group) learning rates, respectively; r_1 and r_2 are uniformly distributed random numbers in the range 0 to 1; and θ is known as the inertial weight and is calculated by

$$\theta = \theta_{max} - (\frac{\theta_{max} - \theta_{min}}{i_{max}})i \tag{3}$$

where $\theta_{\max}$ and $\theta_{\min}$ are the initial and final values of the inertia weight, respectively, and $i_{\max}$ is the maximum number of iterations. The values of $\theta_{\max} = 0.9$ and $\theta_{\min} = 0.4$ are commonly used [10].

Having the velocities of all particles, the position of each particle is

$$\boldsymbol{X}_j^i = \boldsymbol{X}_j^{i-1} + \boldsymbol{V}_j^i \tag{4}$$

This iterative procedure continues until a convergence criterion is met (e.g., the difference between the global best fitness of the last two iterations is smaller than a certain value, or the global best fitness does not change after a certain number of iterations).

Note that other derivative-free optimization algorithms such as genetic algorithms, simulated annealing, ant colony optimization, fuzzy optimization, and neural-network-based methods may also be used to determine the optimum deposition angle.

Rastering orientation optimization

The objective function to be minimized is the maximum error which is a function of rastering orientation. Two different approaches could be made to minimize the horizontal errors: (1) optimizing the orientation of the part in 3D space while the rasters remain in the same direction, and (2) maintaining part orientation constant while optimizing the rastering orientation separately for each layer.

In the first method, the following unconstrained optimization problem is solved

$$minimize\ e_{max}^{part}(\varphi, \theta, \psi) \tag{5}$$

where e_{max}^{part} is the maximum horizontal error for the entire part, and φ, θ and ψ are the rotation angles of the part around x, y and z axes, respectively. The rasters are in the horizontal plane along the y direction. The iteration starts with a population of random values for the three angles. The maximum error for the entire part for each set of angles is calculated using the algorithm explained in the "error estimation algorithm" section. Based on these values PSO determines the next set of angles. This procedure continues until the optimum orientation is found for the part.

In the second approach, the part orientation is unchanged, and, for each layer, the optimum rastering angle, α^k, is determined to minimize the maximum error. Since the rasters are assumed to be horizontal, only one angle is enough to determine their orientation in space. The unconstrained optimization problem is

$$minimize\ e_{max}^{k}(\alpha^k) \quad k = 1, 2, \dots, M \tag{6}$$

where k denotes layer number and M is the total number of layers. For the k^{th} layer, initially, a population of random values is generated and corresponding errors are calculated using the algorithm explained in "error estimation algorithm" section. These values are then utilized in the second iteration to calculate the next angles via PSO, and the procedure is repeated until a convergence criterion is met. The same process is carried out for k+1th layer until each layer is rastered at an optimal angle.

The first approach might be more effective in some cases (e.g., a 2.5D part could be aligned in such a way that all the layers have a rectangular boundary and errors are virtually zero). However, by changing the part orientation, vertical errors will also be affected and a dramatic increase in their values might be possible. The second method, on the other hand, does not alter the vertical errors. Thus, one of the methods described in the introduction section [2-8] could be first employed to determine the optimal part orientation to minimize the vertical errors, and then the proposed approach here could be used to minimize the horizontal errors without affecting the vertical errors. Moreover, the second method deals with each layer separately and independently, so the number of parameters to be optimized, i.e., the degrees of freedom, is equal to the number of layers whereas in the first method, there are only three parameters to manipulate.

Accordingly, the second approach was chosen and the rastering direction was optimized for each layer independently in order to minimize the horizontal errors. Table 1 represents the parameters used in PSO.

Table 1. Parameters used in PSO.

Maximum number of iterations (i_{max})	100
Population size (N)	10
Cognitive (individual) learning rates (c_1)	2
Social (group) learning rates (c_2)	2
Initial value of the inertia weight (θ_{max})	0.9
Final value of the inertia weight (θ_{min})	0.4
Change in global best for termination (mm^2)	0.00001

Case studies

Spur gear

A spur gear (Figure 4) is considered in the first case study and lines of 0.9 mm width are chosen to raster the part. The initial rastering orientation is shown in Figure 5 (left) where the maximum error is 1.794 mm^2. Figure 6 illustrates how PSO converges to the optimal value in 35 iterations. The optimum rastering orientation for spur gear is 157.47° CW which results in 0.370 mm^2 error (see Figure 5 (right)). Thus, optimizing the rastering orientation results in a **79.4% reduction** in maximum horizontal error for this spur gear.

It should be noted that since only the rastering orientation is changed, the travelling distance of the table remains constant for each layer and for the entire part. Thus, the fabrication time does not change. Furthermore, the orientation of the part in 3D space is not altered. Hence, the amount of support material and the number of layers are the same as the original values.

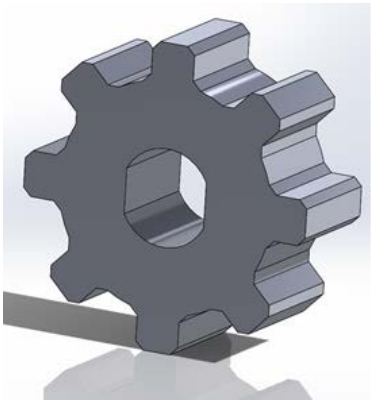

Figure 4. The spur gear used in the first case study.

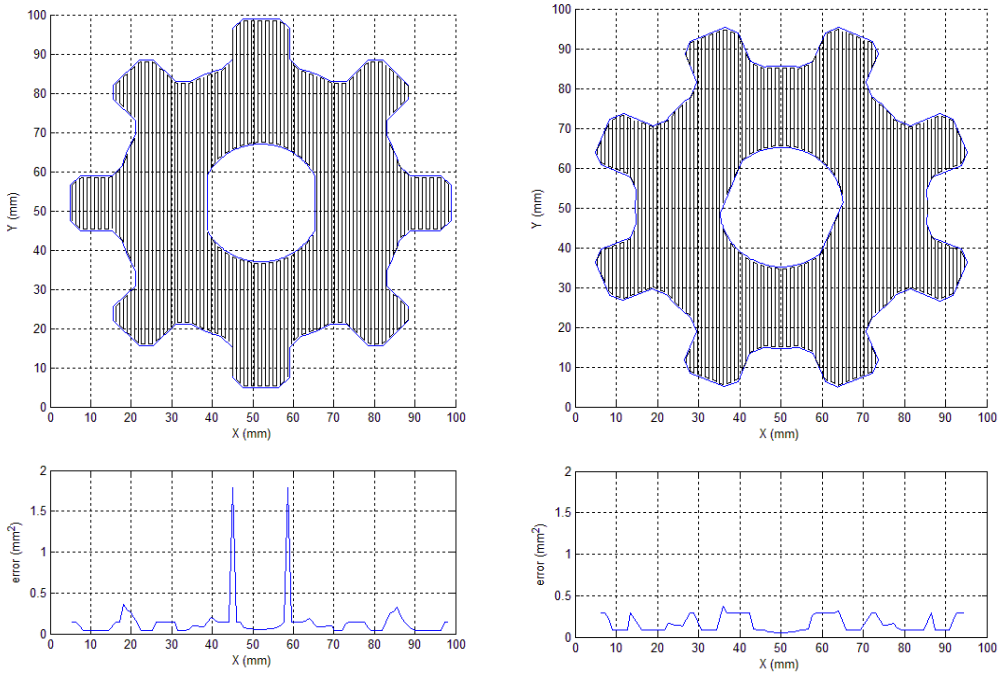

Figure 5. Original (left) versus optimal (right) rastering orientation along with error values for a layer of the spur gear. In the right picture, the orientation of the "part" is the same as the left picture and the rastering direction is changed by 157.47° CW. However, for convenience in illustrating the error diagram, the picture is drawn as if the part is rotated 157.47° CCW.

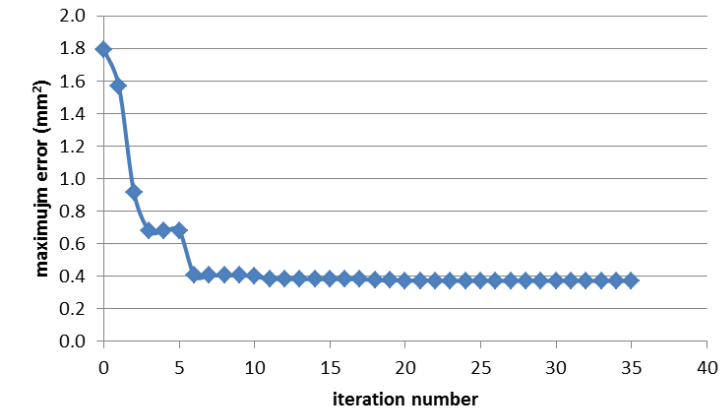

Figure 6. Maximum error versus. number of iterations for a layer of the spur gear.

Liner block

A liner block with embedded sensors is considered in the second case study. Figure 7 shows the liner block with two vertical and two horizontal cavities for sensors. Figures 8-11 show how efficacious the optimal rastering orientation is in reducing the horizontal staircase effect for representative layers of the liner block. In all figures, the orientation of the "part" in the right picture is the same as that in the left picture and rastering direction is changed CW. However, for convenience in illustrating the error diagram, the picture is drawn as if the part is rotated CCW.

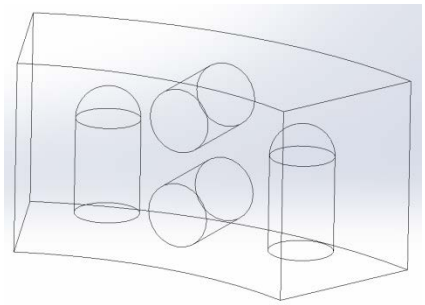

Figure 7. Liner block with two vertical and two horizontal cavities for sensors used as the second case study.

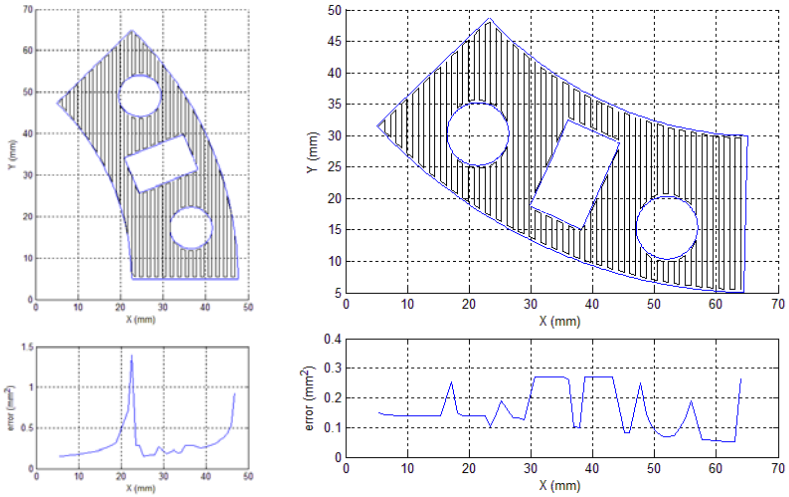

Figure 8. Original (left) versus optimal (right) rastering orientation along with error values for 10th layer of liner block. Optimum rastering orientation is 223.37° CW.

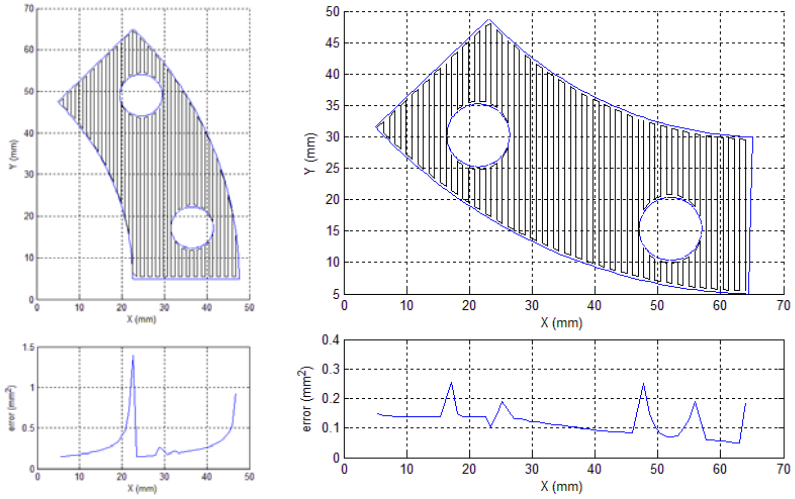

Figure 9. Original (left) versus optimal (right) rastering orientation along with error values for 30th layer of liner block. Optimum rastering orientation is 223.39° CW.

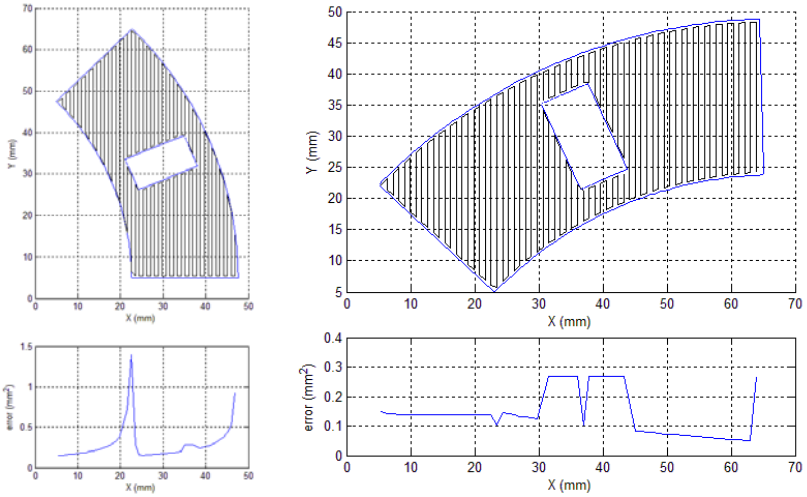

Figure 10. Original (left) versus optimal (right) rastering orientation along with error values for 50th layer of liner block. Optimum rastering orientation is 91.63° CW.

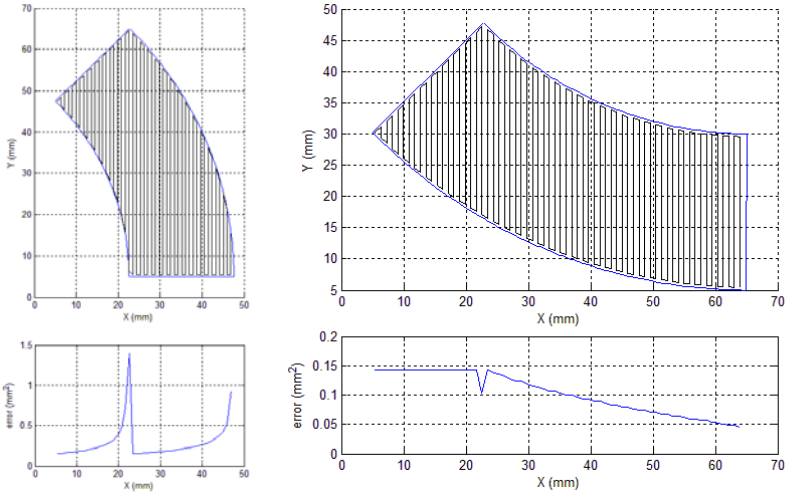

Figure 11. Original (left) versus optimal (right) rastering orientation along with error values for 70th layer of liner block. Optimum rastering orientation is 224.68° CW.

Table 2 compares the error values between the original orientation and the optimal orientation for those representative layers as well as the entire part. The original rastering orientation results in a maximum error of

1.396 mm^2 for all layers, whereas optimal orientations reduce these errors to 0.269, 0.254, 0.269 and 0.143 mm^2 for 10^{th}, 30^{th}, 50^{th} and 70^{th} layer, respectively.

Table 2. Maximum errors of representative layers of liner block in original and optimal rastering directions.

Layer no.	Original orientation	Original error (mm^2)	Optimal orientation	Optimal error (mm^2)	Reduction (%)
10	0°	1.396	223.37°	0.269	**80.7**
30	0°	1.396	223.39°	0.254	**81.8**
50	0°	1.396	91.63°	0.269	**80.7**
70	0°	1.396	224.68°	0.143	**89.8**
Entire part	0°	1.396	223.37°	0.269	**80.7**

The liner blocks were built using a freeform extrusion fabrication process at different orientations as illustrated in Figure 12. In the top two pictures, large staircase errors can be visually observed for both horizontal and vertical cavities. These errors might affect the performance of the embedded sensors. In the bottom pictures, the errors are reduced by choosing suitable rastering orientations.

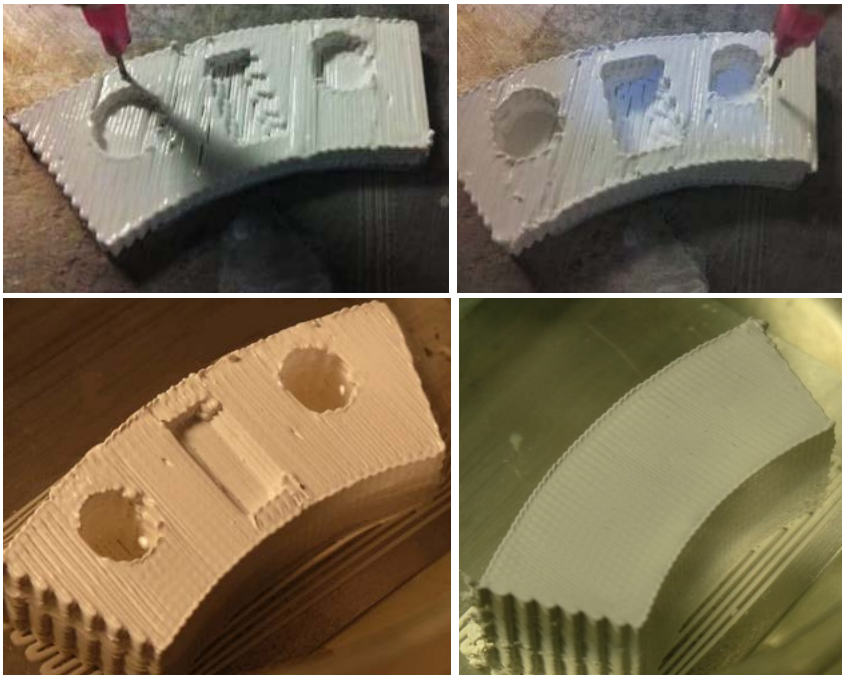

Figure 12. Liner blocks fabricated at different rastering angles.

Summary and Conclusions

The horizontal staircase effect, resulting from approximating a complex layer boundary and its interior by cuboid lines, was considered in this paper. An area deviation criterion was developed to estimate this effect for every line of a layer for an arbitrary object. It was then demonstrated that the direction of the lines has a significant influence on horizontal errors. Therefore, a derivative-free optimization method was utilized to determine the optimum orientation of rasters for each layer of a part to minimize the error.

Two cases were studied to investigate the efficacy of the proposed approach. In the first case, optimizing the rastering orientation of a spur gear resulted in a 79.4% reduction in maximum error. A liner block with embedded sensors was examined next. Depending on the geometry of each layer, the maximum errors were reduced between 80.7 to 89.8%. This part was also printed at various orientations using a freeform extrusion fabrication process.

According to the results, it could be concluded that the proposed approach is effective in reducing the horizontal staircase errors without altering any other performance factors such as the vertical errors, fabrication time, amount of support material, and number of layers.

Acknowledgements

The authors gratefully acknowledge the financial supports by the National Energy Technology Laboratory of the U.S. Department of Energy's Office of Fossil Energy under the contract DE-FE0012272, and the Intelligent Systems Center at the Missouri University of Science and Technology.

References

[1] I. Gibson, D. W. Rosen, and B. Stucker, *Additive Manufacturing Technologies*. Springer, 2010.

[2] W. Cheng, J. Y. H. Fuh, A. Y. C. Nee, Y. S. Wong, H. T. Loh, and T. Miyajawa, "Multi-objective optimization of part-building orientation in stereolithography," *Rapid Prototyp. J.*, vol. 1, no. 4, pp. 12–23, 1995.

[3] P. Alexander, S. Allen, and D. Dutta, "Part orientation and build cost determination in layered manufacturing," *Comput. Aided Des.*, vol. 30, no. 5, pp. 343–356, 1998.

[4] K. Thrimurthulu, P. M. Pandey, and N. V. Reddy, "Optimum part deposition orientation in fused deposition modeling," *Int. J. Mach. Tools Manuf.*, vol. 44, no. 6, pp. 585–594, 2004.

[5] V. Canellidis, J. Giannatsis, and V. Dedoussis, "Genetic-algorithm-based multi-objective optimization of the build orientation in stereolithography," *Int. J. Adv. Manuf. Technol.*, vol. 45, no. 7–8, pp. 714–730, 2009.

[6] A. M. Phatak and S. S. Pande, "Optimum part orientation in Rapid Prototyping using genetic algorithm," *J. Manuf. Syst.*, vol. 31, no. 4, pp. 395–402, 2012.

[7] R. Paul and S. Anand, "Optimal part orientation in Rapid Manufacturing process for achieving geometric tolerances," *J. Manuf. Syst.*, vol. 30, no. 4, pp. 214–222, 2011.

[8] R. Paul and S. Anand, "Optimization of layered manufacturing process for reducing form errors with minimal support structures," *J. Manuf. Syst.*, 2014.

[9] J. Kennedy and R. C. Eberhart, "Particle Swarm Optimization," in *IEEE International Conference on Neural Networks*, 1995, pp. 1942–1948.

[10] S. S. Rao, *Engineering optimization: theory and practice*, 4th ed. John Wiley & Sons, 2009.